Journal of the American Heart Association

PROTOCOL

Study Protocol for HeartMagic: A Prospective Observational Cohort Characterizing Subtypes of Heart Failure With Preserved Ejection Fraction

Philippe Meyer, MD; Angela Rocca, MSc; Jaume Banus, PhD; Augustin C. Ogier, PhD; Costa Georgantas, MSc; Pauline Calarnou, MSc; Anam Fatima, MSc; Jean-Paul Vallée, MD, PhD; Jean-François Deux, MD; Aurélien Thomas, PhD; Julien Marquis, PhD; Pierre Monney, MD; Henri Lu, MD; Alessandra Pia Porretta, MD; Jean-Baptiste Ledoux, MSc; Cloé Tillier, RN; Lindsey A Crowe, PhD; Tamila Abdurashidova, MD; Jonas Richiardi, PhD; Roger Hullin, MD; Ruud B. van Heeswijk, PhD

BACKGROUND: Heart failure (HF) is a life-threatening syndrome with significant morbidity and mortality. Although evidence-based drug treatments have effectively reduced morbidity and mortality in HF with reduced ejection fraction (EF), few therapies have been demonstrated to improve outcomes in HF with preserved EF. This may be caused by the existence of several HF with preserved EF subtypes that each need different treatments. There is therefore an unmet need for a comprehensive approach to subtype patients with HF with preserved EF. This protocol details the approach employed in the HeartMagic (Heart Failure Studied With a Machine Learning, Genomics, and Imaging Combination) study to address this gap.

METHODS: This prospective multicenter observational cohort study will include 500 consecutive patients with HF with preserved EF at 2 Swiss university hospitals, along with 50 age-matched patients with HF with reduced EF and 50 healthy controls. In addition to routine clinical workup, participants undergo genomic, transcriptomic, and metabolomic analyses, and the anatomy, composition, and function of the heart are quantified by comprehensive echocardiography and magnetic resonance imaging. Quantitative magnetic resonance imaging is also applied to characterize the kidney. The primary outcome is a composite of 1-year cardiovascular mortality or rehospitalization. Machine learning–based multimodal clustering will be employed to identify distinct HF with preserved EF subtypes. Statistical analysis will include group comparisons, survival analysis, and integrative multimodal clustering combining clinical, imaging, ECG, genomic, transcriptomic, and metabolomic data to identify and validate HF with preserved EF subtypes.

CONCLUSIONS: The integration of comprehensive magnetic resonance imaging with extensive genomic and metabolomic profiling in this study will result in an unprecedented panoramic view of HF with preserved EF and help distinguish functional subgroups, which may provide a basis for personalized therapies.

Key Words: echocardiography ■ genomics ■ heart failure ■ HFpEF ■ machine learning ■ metabolomics ■ quantitative MRI

Correspondence to: Ruud B. van Heeswijk, PhD, Department of Radiology, Lausanne University Hospital (CHUV), Rue du Bugnon 46, RAD BH08.084, Lausanne 1011, Switzerland. Email: ruud.mri@gmail.com

This article was sent to Sula Mazimba, MD, MPH, Associate Editor, for review by expert referees, editorial decision, and final disposition.

Preprint posted on MedRxiv September 16, 2025. doi: https://doi.org/10.1101/2025.04.10.25325567.

Supplemental Material is available at https://www.ahajournals.org/doi/suppl/10.1161/JAHA.125.043541

For Sources of Funding and Disclosures, see page 12.

JAHA is available at: www.ahajournals.org/journal/jaha

Nonstandard Abbreviations and Acronyms

CHUV	Centre Hospitalier Universitaire Vaudois (Lausanne University Hospital)
HFpEF	heart failure with preserved ejection fraction
HFrEF	heart failure with reduced ejection fraction
HUG	Hôpitaux Universitaires de Genève (Geneva University Hospitals)
ML	machine learning
PARMANav	Parametric Radial Mapping With Respiratory Navigation
UKB	UK Biobank

Heart failure (HF) is a major public health concern that leads to substantial morbidity, mortality, and health care costs, with a prevalence nearing 3% of the general population in most European countries.[1] HF is classified into 3 categories based on left-ventricular ejection fraction (LVEF): HF with reduced EF (HFrEF) when LVEF is ≤40%, HF with mildly reduced EF when LVEF is between 41% and 49%, and HF with preserved EF (HFpEF) when LVEF is ≥50%.[2,3] Over the past 30 years, HFpEF has become the most prevalent HF phenotype in Western countries, now accounting for >50% of cases.[1,4] The prognosis of patients hospitalized for HFpEF is poor, with reported 1-year all-cause mortality rates of ~20% to 25% and rehospitalization rates approaching 50%.[1]

Many patients presenting with HF and an LVEF ≥50% exhibit specific cardiac conditions, such as infiltrative, hypertrophic, or restrictive cardiomyopathy, as well as valvular or pericardial diseases, which are now referred to as HFpEF mimics[5] or secondary HFpEF.[6] Diagnosis of HFpEF should therefore exclude these mimics. However, earlier HFpEF studies may have inadvertently included such patients,[7] and even recent cohorts may still include misclassified cases due to incomplete investigation in older patients.

RATIONALE

Even when mimics are excluded, HFpEF remains a heterogeneous syndrome.[6] Traditionally, LV diastolic dysfunction has been considered central, with increased LV filling pressures and reduced cardiac output at rest or during exercise. More recently, systemic endothelial inflammation, driven by comorbidities such as hypertension, obesity, diabetes, chronic obstructive pulmonary disease, sedentary lifestyle, or iron deficiency, has emerged as a unifying concept.[8–10] This inflammation is linked to myocardial fibrosis, oxidative stress, and signaling pathway alterations that affect cardiomyocyte function.

Beyond diastolic dysfunction, other mechanisms contribute to HFpEF, including LV systolic dysfunction, impaired left atrial function, pulmonary vascular disease, right ventricular dysfunction, systemic arterial stiffening, coronary and peripheral microvascular dysfunction, chronotropic incompetence, skeletal muscle dysfunction, and arrhythmias, especially atrial fibrillation.[11,12]

Despite numerous large phase 3 clinical trials, most pharmacologic interventions have failed to demonstrate clear benefit in HFpEF.[13] Although SGLT2 (sodium-glucose cotransporter-2) inhibitors and the mineralocorticoid receptor antagonist finerenone have shown promise in HF with mildly reduced EF and HFpEF,[14–16] no trial has yet demonstrated a significant reduction in overall or cardiovascular mortality in HFpEF.[17] This may be due to underlying pathophysiological heterogeneity,[6,18,19] inclusion of HFpEF mimics,[7] or the slow progression of the disease that requires longer study durations.[18]

Efforts by major societies, including the Heart Failure Association of the European Society of Cardiology, have focused on defining phenotypes to guide targeted therapies.[6] The Heart Failure Association algorithm proposes 7 HFpEF phenotypes with corresponding treatment strategies. Examples of phenotype-specific treatments include semaglutide (a GLP-1 [glucagon-like peptide-1] receptor agonist) and tirzepatide (a GLP-1 and GIP [glucose-dependent insulinotropic polypeptide] agonist), which have recently shown promise in treating the obese phenotype of patients with HFpEF.[20–23] However, substantial phenotype overlap limits the precision of such classifications. New strategies that extend beyond routine clinical data are therefore necessary to fully capture the complex heterogeneity of HFpEF disease.

OBJECTIVES

This observational study, named HeartMagic (Heart Failure Studied With a Machine Learning, Genomics, and Imaging Combination), aims to perform comprehensive subtyping of patients with HFpEF using a multimodal, integrative approach. By combining clinical data with genomics, metabolomics, and advanced cardiac magnetic resonance imaging (MRI), we will generate a rich, high-dimensional data set.[13] MRI enables detailed quantification of cardiac structure, function, hemodynamics, and tissue composition,[24] and omics data provide insights into underlying molecular mechanisms. Together, these data form an ideal foundation for the application of machine learning (ML) models, which have shown transformative potential in health care by uncovering complex patterns and enhancing predictive accuracy.[25]

Our objective is therefore to identify clinically meaningful HFpEF subtypes linked to distinct pathophysiological mechanisms and outcomes. We aim to build one of the largest and most comprehensive HFpEF cohorts to date, supporting the development of more targeted and effective therapeutic strategies. This protocol outlines the methods used across all modalities.

METHODS

Study Design

It is planned to make all data available in a public repository after anonymization; this is detailed in the informed consent forms that all participants signed. This prospective observational clinical study will not interfere with standard care, and no randomization is required. A total of 500 consecutive patients with current or recent hospitalization for acute heart failure and preserved LVEF at the Geneva University Hospitals (HUG) or the Lausanne University Hospital (CHUV) will be enrolled, along with 50 patients with HF with reduced LVEF and 50 age-matched healthy controls (Figure 1). The latter 2 groups will serve only as reference groups to enable comparison and calibration of multimodal analyses, whereas the primary aim of the study is to subtype patients with HFpEF. These comparator groups will thus not be further stratified. Recruitment is planned over a 3-year period based on acute HF hospitalization rates at both centers. Each participant will undergo genetic, genomic, and metabolomic analyses; comprehensive echocardiography; and quantitative MRI. Patients with HF will receive a follow-up by phone at 30 days, 90 days and 1 year post discharge.

Setting

The study is conducted at 2 Swiss academic centers: the HUG and the CHUV. HUG has ~2000 beds, and CHUV has ~1500 beds. Both are tertiary care facilities that serve a population of >2 million people across their respective regions. Each year, ~1200 patients are hospitalized for acute heart failure at HUG, and CHUV admits ~700 patients for the same condition, according to the Swiss Federal Office of Statistics.

Patients

Ethics approval was obtained from the Ethics Committee of the Canton of Vaud of Switzerland under number 2022–00934. All participants provide written informed consent to participate before enrollment. The study will prospectively include 500 patients with HFpEF, while simultaneously recruiting 50 patients with HFrEF and 50 healthy participants, age- and sex-matched to the group with HFpEF (Table 1). The latter 2 groups will serve as reference groups to enable comparison and calibration of multimodal analyses, whereas the primary aim of the study is to subtype patients with HFpEF.

Table 1. Expected Distribution of Recruitment Across the 2 Sites

	CHUV	HUG	Total
Patients with HF and preserved EF	290	210	500
Patients with HF and reduced EF	30	20	50
“Healthy” volunteers	30	20	50
	350	250	600

CHUV indicates Centre Hospitalier Universitaire Vaudois (Lausanne University Hospital);EF, ejection fraction; HF, heart failure; and HUG, Hôpitaux Universitaires de Genève (Geneva University Hospitals).

For patients with HFpEF the inclusion criteria are:

1. Adult ≥18 years old
2. Written and informed consent
3. Presence of dyspnea
4. Current or recent hospitalization for acute HF with signs of pulmonary or systemic congestion
5. On diuretic treatment before enrollment
6. LVEF ≥50% on echocardiography with at least 1 structural or functional cardiac abnormality compatible with HFpEF according to the current HFpEF definition.[3,26]

The exclusion criteria are:

1. Claustrophobia, ferromagnetic implants, or any other contraindications to MRI
2. Contraindication to adenosine/regadenoson or gadolinium-based contrast agents
3. Pregnant or breastfeeding women
4. Alternative causes of dyspnea: valvular dysfunction considered by the investigators to be clinically significant, anemia with hemoglobin <10 g/dL, severe pulmonary disease
5. Chronic inflammatory disease of systemic or rheumatic origin
6. Cardiac amyloidosis or other infiltrative cardiac disease, sarcomeric hypertrophic cardiomyopathy, pericardial constriction
7. Occurrence of any of the following before enrollment:
   a Acute inflammatory heart disease (eg, myocarditis, endocarditis) within 90 days
   b Myocardial infarction within 90 days
   c Coronary artery bypass graft surgery within 90 days
   d Percutaneous coronary intervention within 30 days

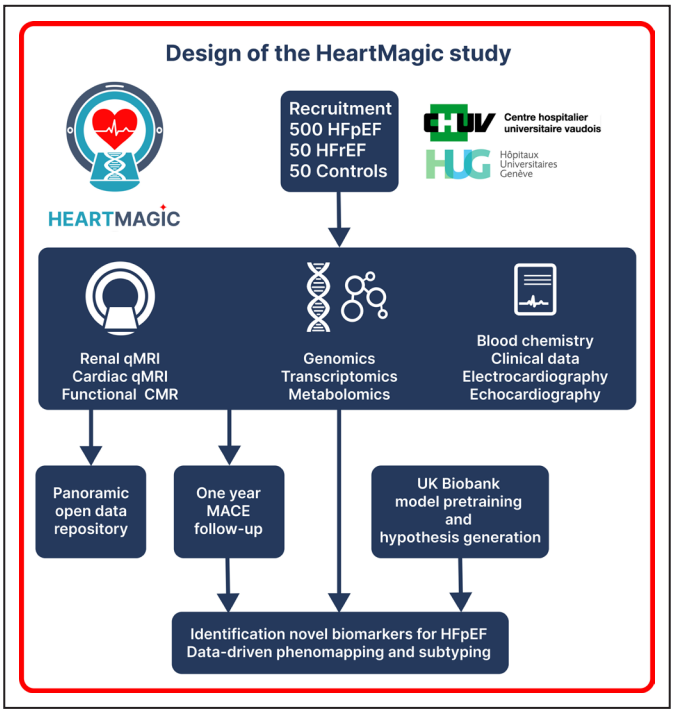

Figure 1. Setup and design of the HeartMagic study.

e Stroke or transient ischaemic attack within 90 days
8. Comorbid conditions associated with life expectancy <1 year
9. Alcohol abuse
10. Liver cirrhosis classified as Child–Pugh C
11. Severe chronic kidney disease with estimated glomerular filtration rate <30 mL/min per 1.73 m^2
12. Incapacity of judgment
13. Active COVID-19 infection
14. Unwillingness to receive notice of accidental findings
15. A body size prohibitive for the 60 cm-diameter bore of the MR scanner

Patients with HFrEF are age- and sex-matched with patients with HFpEF and share similar inclusion criteria, except for an LVEF <40%, as well as comparable exclusion criteria. Healthy volunteers (aged ≥60 years) must have NT-proBNP (N-terminal pro-B-type natriuretic peptide) levels at or below the age-adjusted upper limit and no history of cardiac disease or more than moderate hepatic disease. They are also age- and sex-matched with the group with HFpEF and share similar exclusion criteria with the other 2 groups.

Recruitment

Patients hospitalized for dyspnea at the emergency department are screened for eligibility. The screening process includes an evaluation of HF symptoms and signs, underlying cause, past medical history, initial blood test results, echocardiographic evaluation of LVEF, and the potential presence of cardiovascular implantable electronic devices and other ferromagnetic materials. Patients who meet the inclusion criteria are approached after their referral to the internal medicine and cardiology wards. They receive detailed information about the study and an informed consent form, with up to 48 hours allowed for consideration and decision-making.

The scheduled enrollment of 500 patients with HFpEF, 50 patients with HFrEF, and 50 healthy controls is expected to be complete by the end of 2026. All 3 participant groups will be recruited simultaneously. Weekly surveillance of age and sex distribution among recruited patients will be performed to document representativeness. Based on epidemiological data, we anticipate a female-to-male ratio of approximately 2:1 in HFpEF and 1:4 in HFrEF, but no predefined sex ratio will be enforced. For the HFrEF and healthy control groups, we will aim to maintain broadly comparable distributions to facilitate interpretability.

Age-matched healthy controls are recruited via the University for Seniors in Lausanne and Geneva through online advertisement. Interested individuals attend an informational session, complete the informed consent process, and receive a compensation of CHF 200.

Patient Study Procedure

Each patient is invited to remain in follow-up for up to 1 year after inclusion, which aims to document routine care. The study procedures are divided into 3 parts (Figure 2):

1. Enrollment and information visit: the patient receives information about the study's purpose, procedures, risks, and benefits. After reviewing and discussing the informed consent form, the patient has the opportunity to ask questions before deciding to participate. If the patient agrees, they sign the informed consent form, and the next steps are arranged.
2. Baseline visit (day 1): blood (~40 mL) is collected. Transthoracic echocardiography and cardiac MRI are also performed on the same day.
3. Follow-up at days 30, 90, and 365: follow-up is conducted by phone and documents patient-related outcomes (morbidity, mortality, health status changes), which are validated through review of medical documentation in a second step. If a health issue has arisen, the participant is invited for an additional ambulatory visit at CHUV/HUG.

Blood Sampling

Blood samples are collected for the analysis of metabolomics, genomics, transcriptomics, and clinical chemistry. After cubital venipuncture, specific tubes are filled for each type of analyses. Blood for clinical chemistry and hemogram analyses are processed by the local departments of laboratory medicine (Table S1). Samples for other analyses are aliquoted, frozen, and stored at −80 °C, and later sent in batches of 96 samples to specific laboratories. The assessment of blood parameters associated with systemic inflammation uses the human proinflammatory panel I (MESO SCALE DISCOVERY) cytokine assay (K15052D), which measures IFNγ (interferon γ), IL-1ß (interleukin-1ß), IL-6 (interleukin-6), IL-10 (interleukin-10), and TNFα (tumor necrosis factor α).[27] Additional aliquots of plasma and serum will be stored at −80 °C for potential future analyses, including measurement of novel biomarkers.

Metabolomics

A total of 2.5 mL of whole blood is collected in lithium heparin tubes and centrifuged to obtain plasma, which is aliquoted into tubes suitable for −80 °C storage. Samples are sent in batches of 96 to the University Center for Legal Medicine of Lausanne and Geneva for analysis. Metabolites are extracted from 100 µL of plasma using a cold methanol-ethanol-water (2:2:1) solvent mixture. Samples are analyzed in full scan mode (positive and negative polarities) using ultra-high-performance liquid chromatography coupled with a Thermo Scientific high-resolution Exploris 120 mass spectrometer in RP (Kinetex C18, in positive and negative modes). Separation is performed in gradient elution mode with mobile phases in positive mode (H2O; 0.1% formic acid and MeOH; 0.1% formic acid) and in negative mode (H2O; 5 mM Ammonium acetate +0.25 mM Ammonium fluoride and MeOH). This will allow detection of several thousand metabolite features, as described previously.[28,29] The expected overlap of compounds between the different approaches is used as an internal validation to assess the adequacy of our results. Raw ultra performance liquid chromatography-high-resolution mass spectrometer data are processed using Compound Discover 3.3 software for peak detection, chromatogram alignment, and isotope annotation. To provide the highest quality

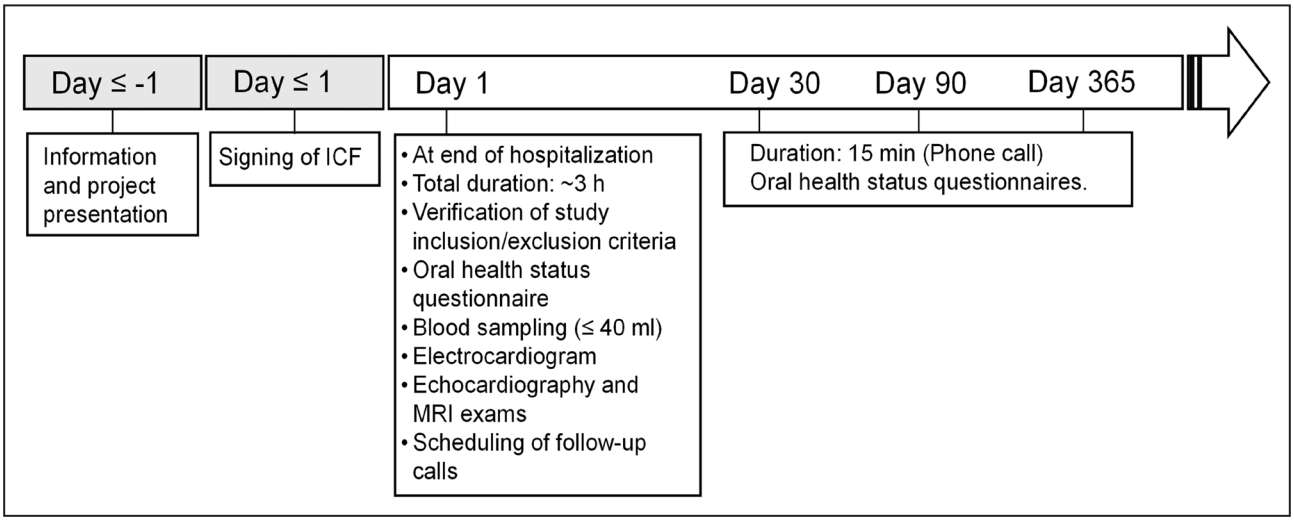

Figure 2. Flow chart of the study procedure.
ICF, informed consent form; and MRI, magnetic resonance imaging.

data for bioinformatics mining, quality controls (ie, representative pool of samples) and internal standards are used to assess overtime-analytical drift (ie, batch effects).[30] To tackle this issue, we will use a method called systematic error removal using random forest and "Dbnorm," which includes algorithms for preprocessing and removing technical heterogeneity from the data via a statistical model in a 2-stage procedure.[31] The determination of the metabolomic signature has the potential to highlight discriminant metabolites significantly different between subtypes of the HFpEF umbrella.

Over the past few years, several large-scale metabolomics studies on thousands of biological samples have been performed on the platform described.[32,33] The human metabolome has not been completely covered, nonetheless, the discriminant metabolites will be characterized using both their MSn fragmentation pattern and open-access libraries.[34] With accurate mass measurement, a homemade script will first be used to identify discriminant metabolites according to a predefined m/z list of metabolites. This list, including ~5000 present or detected metabolites in biofluids, is built from the human metabolome database and updated from our own library. We additionally use the human metabolome database (www.hmdb.ca), lipidmaps (www.lipidmaps.org), metlin (http://metlin.scripps.edu/index.php), and mzcloud (www.mzcloud.org), totaling >40 000 entries. Metabolite identification will also be then performed using SIRIUS 4.7.4, a software that determines the most likely elemental composition of metabolites through the analysis of isotopic patterns and tandem mass spectrometry fragmentation spectra, and CANOPUS, a computational tool for systematic annotation of compound chemical classes.[35,36]

Genomics

A total of 1.2 mL of whole blood is collected in EDTA-K3E tubes, aliquoted into tubes suitable for −80 °C storage, and sent in batches of 96 to INRAE (the French National Research Institute for Agriculture, Food, and Environment; Paris, France) for DNA extraction and genotyping. Each batch includes a mix of samples from patients with HFpEF, patients with HFrEF, and controls. Genotyping is performed on the GENTYANE INRAE Clermont platform (UMR GDEC no. 1095 INRAE/UCA, https://gentyane.clermont.inrae.fr/) using the Axiom Precision Medicine Diversity Array (Thermo Fisher Scientific, Waltham, MA, USA). This array provides >93% marker overlap with the UK Biobank (UKB) Axiom array in the categories of interest for polygenic risk scores (discussed later), and >800K markers in the imputation grid, ensuring that we can match with UKB genomic data. Data are provided in CEL format.

Transcriptomics

For gene expression, 2.5 mL of whole blood is stored in PAXgene tubes at −80 °C, and sent to QiaGen (Hilden, Germany) on dry ice for RNA extraction. Sequencing is performed at the Lausanne Genomic Technologies Facility, University of Lausanne, Switzerland (https://www.unil.ch/gtf). Sequencing libraries are prepared from 500 ng of total RNA using the Illumina Stranded mRNA kit from Illumina. Globin depletion is performed using the FastSelect kit from Qiagen. Sequencing is carried out on an Aviti sequencer (Element Biosciences, San Diego, CA, USA) using single-end sequencing with 150 cycles, at a coverage of 25M reads per sample. Sequencing data are demultiplexed using the Bases2Fastq 2.0 software, quality checked using Fastqc v0.11.9 (https://www.bioinformatics.babraham.ac.uk/projects/fastqc/) and Fastq Screen,[37] and finally provided in FASTQ format.

Use of ECG

ECGs are digitally stored and analyzed using the validated BRAVO and GLASGOW algorithms,[38–40] enabling extraction of >300 quantitative features for detailed electrical phenotyping. These high-dimensional data will be integrated with imaging and genomic data sets for advanced analyses, including deep learning–based approaches and genome-wide association studies. In addition, the Transformer-based polygenic risk score approach will be explored to model complex genotype–phenotype relationships. In this approach, we propose to use an 8-layer prenorm transformer architecture to modify single-nucleotide polymorphism effect estimates from linear methods and from a covariate model. After thresholding out low-effect size single-nucleotide polymorphisms, they will be combined into blocks of 2048, mapped, and then concatenated with covariates before being fed to the transformer. After decoding to recover the original dimensions, the modified effect sizes will be summed to form a single scalar, added to the output of the covariate model, and the loss with respect to the ground truth continuous phenotype will be computed with a smooth L1 norm.[41]

Transthoracic Echocardiography

Transthoracic echocardiography is routinely performed once patients are euvolemic and comfortable in the supine position. All exams are conducted on an Epiq CVx-3-dimensional (3D) Ultrasound system (Philips Healthcare, Eindhoven, the Netherlands) using an X5-1c 3D transthoracic probe. A comprehensive 2-dimensional (2D) examination is performed initially.[42] Additionally, 3D acquisitions of the left ventricle and left atrium are obtained using the Dynamic Heart Model automated 3D tool (Philips Healthcare, Eindhoven, the

Netherlands), and 3D images of the right ventricle are captured using the 3D-autoRV tool (Philips Healthcare, Eindhoven, the Netherlands). Longitudinal strain of the left ventricle, left atrium, and right ventricular free wall is assessed using the Autostrain LV, Autostrain LA, and Autostrain RV postprocessing tools, respectively (Philips Healthcare, Eindhoven, the Netherlands). All measurements adhere to the recommendations from the European Association of Cardiovascular Imaging for chamber quantification,[43] evaluation of left ventricular diastolic function,[44] and the European consensus on the diagnosis and imaging of HFpEF.[26,45] Valvular disease is classified as mild, moderate, or severe according to current guidelines.[46–48] The list of echocardiographic measurements is presented in Table S2.

Magnetic Resonance Imaging

Image Acquisition

Study participants are scheduled for a 1-hour MRI exam on a fully CE-marked clinical 3 tesla (T) scanner (Prisma or PrismaFit, Siemens Healthineers, Erlangen, Germany) of the Center for BioMedical Imaging located in the Departments of Radiology of the CHUV and the HUG. Scanning is always performed by a technologist trained for cardiac research scans or a radiologist specialized in cardiac MRI, and a cardiologist is present for the injection of the pharmacological stressor. Besides routine localizer scans, this 1-hour exam subsequently consists of (Table 2, Table S3):

1. Kidney morphology: Coronal and transverse T_2 half-Fourier-acquired single-shot turbo spin echo.[49]
2. Kidney oxygenation: Breath-held coronal blood oxygen level dependent T_2* mapping.[50]
3. Kidney tissue characterization: free-breathing coronal native joint T_1-T_2 mapping (Parametric Radial Mapping With Respiratory Navigation [PARMANav])[51] to quantify interstitial fibrosis and edema.
4. Cardiac function: routine 2D cine of the heart (short-axis stack, 2-chamber, 3-chamber, 4-chamber, and LV outflow tract views).[52]
5. Cardiac flow: 2D flow just above the level of the aortic valve to measure the ejected blood volume.
6. Myocardial tissue characterization: free-breathing 2D native joint T_1-T_2 mapping

Table 2. MRI Pulse Sequence Parameters

Sequence	HASTE	BOLD	PARMANav	2D cine	qPerf	5D FRF	4D flow
Sequence type	Turbo spin echo	Multi-echo GRE	GRE	Balanced steady-state free precession	GRE	GRE	GRE
Dimensions	2D	2D	2D	2D	2D	5D	4D
Echo time, ms	96	6–52	1.5	1.28	0.98	1.33	2.25
Repetition time, ms	1600	76	3.36	3.39	1.99	2.99	4.27
Echoes	205	12	1	1	1	1	1
Flip angle, °	80	30	12	43	14	15	12
Matrix size	256×256	256×256	192×192	256×170	192×114	160×160×160	160×102×39
Field of view, mm^2	280×280	400×400	300×300	380×285	360×270	220×220×220	380×304×120
Slices	10	1	1	1–12	3	—	—
Slice thickness, mm	5	5	8	8	8	1.38	2.5
Acceleration	GRAPPA, PF	—	CS	CS	GRAPPA, PF	CS	GRAPPA/CS
ECG triggering	N	N	Y	Y	Y	N	Y
Retrospective motion compensation	BH	BH	LL-NAV	BH	Free breathing	SN	LL-NAV
Temporal resolution (ms)	—	—	151	Heartbeat/25	227 ms	Heartbeat/25	Heartbeat/25
k-Space trajectory	Cartesian	Cartesian	GA radial	Cartesian	Cartesian	GA-radial	Cartesian
Inline recon	Y	Y	N	Y	Y	N	Y
Acquisition duration	16s	23s	25–40 heartbeat	2–24s	90 heartbeat	4m05s	4m37s–9m
Prep module(s)	—		T_2p, inversion recovery	—	Sat	—	—
Reference	49	50	51	52	53	24	55

BH indicates breath hold; BOLD, blood oxygen level dependent; CS, compressed sensing; FB, free breathing; FRF, free-running framework; GA, golden angle; GRAPPA, GeneRalized Autocalibrating Partial Parallel Acquisition; GRE, gradient-recalled echo; HASTE, half-Fourier-acquired single-shot turbo spin echo; LL-NAV, lung-liver respiratory navigator; MRI, magnetic resonance imaging; PARMANav, Parametric radial mapping with respiratory navigation; PF, partial Fourier; qPerf, quantitative myocardial perfusion imagin; SN, self-navigation; TE, echo time; TR, repetition time; T_2p, T_2 preparation; 2D, 2-dimensional; 4D, 4-dimensional; and 5D, 5-dimensional.

(PARMANav)[51] to quantify interstitial fibrosis and edema at the basal, midventricular, and apical short axis as well as the 4-chamber orientations.
7. Quantitative myocardial stress perfusion[53]: if estimated glomerular filtration rate >30 mL/min per 1.73 m^2, quantitative myocardial perfusion imaging after the injection of a pharmacological stressor (100 mg adenosine or 400 µg regadenoson). Either stressor is applied because they are part of the local protocols; in addition, their effect on the physiologically in equivalent.[54] This is followed by a half-dose of gadolinium-based contrast agent (GBCA): either 0.05 mmol/kg gadobutrol (Gadovist, Bayer AG) or 0.1 mmol/kg gadoteric acid (Dotarem, Guerbet) during the acquisition.
8. Cardiac anatomy and function: A second half-dose of GBCA is immediately followed by free-running 5-dimensional (5D) imaging to assess anatomy and function at isotropic high spatial resolution in addition to the routine 2D cine.
9. Thoracic flow: 4D flow (ie, 3 spatial dimensions over time) imaging to quantify the flow patterns and velocities in the heart and great vessels.[55]
10. Postcontrast myocardial tissue characterization: repetition of the PARMANav free-breathing joint T_1-T_2 mapping 8 to 18 minutes after the injection of the second dose of GBCA, now to quantify the extracellular volume.
11. Quantitative myocardial rest perfusion imaging: the same scan as the stress perfusion imaging, without the stressor and with a third half-dose of GBCA.

After the scan, images and raw k-space data are directly saved to secured servers managed by the CHUV and HUG information technology departments.

Image and Map Reconstruction

Half-Fourier-acquired single-shot turbo spin echo images and blood oxygen level dependent maps of the kidney as well as 2D cine, quantitative myocardial perfusion imaging, and 4-dimensional flow of the heart are reconstructed on the scanner with manufacturer software. Raw data of the PARMANav and 5D free-running framework acquisitions are exported to a separate workstation for image and map reconstruction.

For the PARMANav joint T_1-T_2 maps of both the kidney and heart, source images are reconstructed with compressed sensing.[51,56] The extended phase graph formalism is employed to simulate a dictionary of signals for a broad range of T_1 and T_2 values. This dictionary is acquisition specific and must be generated for each scan, as heart rate and respiratory gating influence magnetization evolution. The reconstructed images are matched pixel by pixel to the closest dictionary entry using a dot product, resulting in T_1 and T_2 maps.

For the free-running 5D images, cardiac and respiratory motion signals are self-gated and extracted from the raw data using the repeated superior–inferior projections of the 3D radial trajectory.[57] Principal component analysis is first applied to separate the respiratory components, and second-order blind identification is used to isolate the cardiac components.[58] A Gaussian fit is applied to the power spectral density of each resulting component to identify the cardiac signals,[59] which favors the extraction of signals with a fundamental frequency within the expected physiological range. These physiological signals are subsequently used to bin the acquired data into cardiac and respiratory phases as previously described,[24] resulting in undersampled 5D data. Respiratory binning is achieved by dividing the respiratory signal into 4 equally populated phases, ranging from end-expiration to end-inspiration. The cardiac signal is used to organize the data into nonoverlapping phases of 50 ms. Finally, a k-t sparse sensitivity encoding compressed sensing algorithm is employed to reconstruct the 5D whole-heart images.[24,60] Cardiac and respiratory regularization weights are set to 0.005 and 0.03, respectively, to ensure optimal reconstruction quality while maintaining the temporal and respiratory coherence of the data.

Clinical Data

We collect data related to hospitalization duration (timing), movements between the services, interventions, medication, and imaging exams from the hospital information systems (Table S4). All clinical data are coded. Participant data from both hospitals are entered into an electronic case report form. The study database is Research Electronic Data Capture (REDCap), hosted on a secure institutional server at CHUV, with protected access.

Statistical Analysis

Overall Strategy

The statistical analysis plan focuses on developing imaging and genomics analysis methods applicable to the UKB, which is our discovery cohort, and applying these methods on our own data to validate our findings. Although UKB is a community sample and not clinically enriched in patients with HFpEF, its large size makes it suitable as a development and discovery data set around heart failure, cardiovascular disease more generally, and HFpEF risk factors. Using the validated H2FPEF risk score as a surrogate for HFpEF diagnosis[61] will be considered, although it is limited by several factors: (1) transthoracic echocardiography is

not available in UKB, leading to a truncated maximum score; and (2) the score is meant to be applied to patients presenting with dyspnea, rather than a generic population. Diagnostic uncertainty is further increased by lack of NT-proBNP values for UKB subjects.

Initially, we will use group comparisons to identify differences in the features obtained from each of the modalities between the different clinical groups available in our data set, as well as unsupervised methods within the group with HFpEF. In a second step, we will resort to survival analysis (time-to-event analysis for the primary outcomes of the study), in particular within the group with HFpEF, to focus on clinically relevant disease subtypes. Finally, we will focus on integrative analysis, where multiple modalities (clinical, imaging, ECG, genomics, transcriptomics, metabolomics, etc) are considered jointly for subtyping.

Sample Size and Power Calculations

For transcriptomic analyses, we estimated statistical power using the R/Bioconductor package RnaSeqSampleSize (v1.17.0).[62] Assuming 20 000 genes, an average of 5 reads per gene, a minimum fold change of 2 between groups, and a false discovery rate of 5%, a sample size of 50 participants per group yields ~80% power to detect differential expression in ~500 predictive genes (preselected from literature or UKB). For smaller effect sizes, such as a fold change of 1.5, power decreases to ~60% under the same assumptions. These calculations indicate that, although the comparator groups (n=50 HFrEF, n=50 controls) are not designed for detailed subgroup analyses, they retain adequate power for validation of candidate biomarkers. For HFpEF outcomes, the larger cohort (n=500) ensures adequate event numbers (≈75 deaths and ≈250 rehospitalizations over 12 months) to support survival analyses and biomarker discovery.

MR Image and Map Analysis

Renal diameter and volume and medullary and cortical thickness and volume are derived from the half-Fourier-acquired single-shot turbo spin echo series. In the renal T_1, T_2, and T_2^* maps the cortex and medulla are automatically segmented with a deep-learning-based 2D U-Net.[63]

In the routine 2D cine images, LV and right ventricular blood and myocardial volumes and mass, LVEF, right ventricular EF, and left atrium and right atrium volumes are manually segmented. The results in the first 100 subjects are then used to train deep learning-based automated segmentation networks for the 2D cines. LV long-axis systolic function is measured using mitral annular systolic excursion and LV global longitudinal strain. Left and right total atrial emptying fraction, passive atrial emptying fraction and active atrial emptying fraction are measured from the maximum left atrium and right atrium volumes, the before atrial contraction and the minimum atrial volumes as reported by Kowallick et al.[64]

We also use these 2D cine data to develop methods to study spatiotemporal patterns. We process the images, segment the ventricles, and divide the myocardium in different regions (16 American Heart Association subsegments for the left ventricle myocardium, 9 segments for the right ventricle myocardium). These divisions give us the flexibility to represent the heart as a spatiotemporal graph in which the nodes represent these myocardium regions and edges represent similarities between segments. Used across multiple acquisition sequences (relaxometry, strain, motion, etc), these structural heart graphs will represent quantitative tissue properties, mechanical properties, and structural properties of the heart using a unified representation. The goal is to identify key functional and anatomical properties that are relevant to quantify the cardiac function and the cardiovascular health. The use of graph neural networks will allow the use of low-dimensional, latent representations of structure and function.

Similarly, from the 5D free-running framework images[24] we extract global measures such as the diastolic and systolic atrial and ventricular volumes, as well as segmental myocardial measures such as wall thickness and strain. To assess the presence of pulmonary hypertension as required by the H_2FPEF score,[61] we calculate the septal-to-free-wall curvature ratio.[65]

Myocardial T_1 and T_2 values are manually segmented on the PARMANav maps according to the standardized 17 American Heart Association LV segments,[66] as well as for their equivalent right ventricular segments where available.[67]

Subendocardial and subepicardial as well transmural myocardial perfusion is quantified in 16 sectors at 3 level (basal, mid, and apical) according to the Kellman method.[68]

In the 4-dimensional flow MRI we measure aortic and pulmonary flow, flow through the atrioventricular and ventriculo-arterial valves, the transmitral flow profile, wall shear stress at the level of the aorta and pulmonary artery, and pulse wave velocity in the aorta. An analysis of the components of intraventricular flow and turbulence in the left atrium are performed on a dedicated software (Cvi 42, Circle, Montreal, Canada). Peak early diastolic tissue velocity (e') is assessed at the septal and lateral mitral annulus using automated mitral valve tracking. Mitral inflow velocities (E and A) are measured and combined with e' to measure the average septal-lateral E/e' ratio reflecting pulmonary capillary wedge pressure. Tricuspid annular plane systolic excursion and peak tricuspid annular systolic

tissue velocity (S′) is measured as indices of right ventricular longitudinal systolic function.

To identify associations between the image-based biomarkers and clinical outcomes we will further develop systematic screening approaches with careful propensity matching and survival analysis[69] to relate these potential biomarkers to clinical outcomes.

Omics Preprocessing and Analysis

For genomic data, we will apply standard quality control and preprocessing[70] including sample quality checks (sex inconsistencies, call rate, etc), marker quality checks (minor allele frequency, Hardy–Weinberg equilibrium), and batch effect analysis and correction, using the bigsnpr package[71] and other in-house tools.

For metabolomic data, after acquisition, preprocessing and quality control steps described previously, we will use the negative and positive mode results separately (~8000 metabolites in total), obtained from untargeted analysis, to narrow down the list to ~200 metabolites for in-depth characterization. This will be done by clinical group comparison, as well as correlation screening with respect to imaging features of interest, survival-linked features of interest, and associations with selected genes and single-nucleotide polymorphisms.

For transcriptomic data, we will run an established quality control pipeline (RNA-SeQC2[72]), annotate to the latest genome assembly, and quantify gene expression using Salmon[73] (using the alternative pipeline of first aligning with STAR[74] and quantifying using HTSeq).[75]

Novel Biomarkers for HFpEF

Each omics will be processed according to modality-specific pipelines as described. For multimodal analysis, our first approach will be to group participants according to one modality (for example, clustering by above- versus below-median cardiovascular MR-derived markers and studying related survival), then examine the distribution of other biomarkers between these groups (for example, metabolomics profiles). To promote early integration of modalities, in our second approach we will construct participant similarity graphs for each modality, where each participant is a node and edges represent pairwise similarity (eg, cosine distance between expression values of candidate genes). Each such similarity graph will be treated as a "layer" in a multilayer graph, and multimodal subtypes will then be defined through community detection algorithms such as the Leiden algorithm. As a baseline benchmark for these approaches, we will use Similarity Network Fusion. The resulting multimodal communities will subsequently be evaluated by survival analysis.

The main focus will be to find biomarkers with outcomes-linked differences within the HFpEF group, in particular using survival analysis ("survival subtypes"). Because the follow-up period is 1 year and the recruitment is ongoing, during the time period where event counts are insufficient for modeling, we will in the initial analysis phase focus instead on unsupervised subtyping ("phenotyping subtypes") and supervised group characterization. Then, when outcomes are observed, clustering results will be evaluated by looking at the silhouette coefficient, the concordance index, normalized mutual information, and the adjusted Rand index with respect to observed primary and secondary clinical outcomes.

Another approach to mitigate the lack of events is to rely on the UKB, a large observational cohort, for hypothesis generation. We use the UKB data set to identify various cardiovascular MR-derived biomarkers that have prognostic value on the risk of hospitalization and death due to HF, as well as for comorbidities associated with HFpEF. These analyses will serve to narrow down the set of candidate biomarkers to a manageable number that can be tested with sufficient power in the HeartMagic cohort. For genomics specifically, we will derive low-dimensional risk scores from genome-wide association studies in UKB and validate them in HeartMagic, thereby ensuring feasibility despite smaller sample sizes.

A focus of the work is imaging genetics using cardiovascular MR-derived imaging phenotype as complex traits and genome-wide association studies targets. Preprocessed genomics data will thus be used for genome-wide association studies analyses (plink tool), in UKB for discovery, and our sample for validation. Although cine and T_1 acquisitions are not the same in both data sets, the approach should allow us to narrow down the set of plausible candidates. From these, we will also generate low-dimensional representations of genomic data, to be included in subtyping analyses, by using our newly proposed transformer-based nonlinear method for polygenic risk scoring.[41]

Throughout, we will use a combination of the omics available to obtain a better understanding of group differences, phenotyping subtypes, and survival subtypes. For example, we will look at consensus across omics and for example, differential gene expression between subtypes obtained from other omics and modalities, although this approach can struggle to exploit discordant relationships.[76] We will also pursue graph-based approaches, viewing the problem as a community detection problem on a multilayer graph.

These analyses aim to produce novel interpretable, predictive, and reproducible biomarkers that can improve clinical decision-making, refine prognostic estimates, and can be used to propose novel treatment

avenues and secondary end points for future clinical trials.

Open Access and Open Data

All studies and substudies will be published in an open access format. All data will be converted to depersonalized nonproprietary formats and will be deposited in Findable, Accessible, Interoperable, Reusable (FAIR) online repositories for open access, except for genomic data, which will be deposited with access control.

Identifying attributes including names and dates of birth will be removed from all data. Then, data will be depersonalized according to its type: tabular data (clinical, blood chemistry, ECG features) will be depersonalized using tools such as ARX[77]; imaging data will be converted to NIfTI before sharing, with potentially sensitive headers removed; sequence reads in transcriptomic data will be sanitized[78,79]; metabolomic data will be shared as is because they are not thought to contain directly identifying information.

DISCUSSION

This study protocol addresses the complex and heterogeneous nature of HFpEF, a prevalent condition with poor prognosis and few effective pharmacological treatments. By integrating advanced MRI with metabolomic, transcriptomic, and genomic analyses, this prospective observational study aims to refine HFpEF subtyping through ML-based multimodal clustering. With a cohort of 500 patients with HFpEF, 50 age-matched patients with HFrEF, and 50 healthy controls, we seek to identify clinically meaningful subgroups linked to distinct pathophysiological mechanisms and clinical outcomes, with a primary composite end point of 1-year cardiovascular mortality or rehospitalization.

ML is central to precision medicine, particularly when applied to rich panoramic data such as genetics, metabolomics, proteomics, and quantitative MRI.[76] This study focuses on 2 ML strategies: integrative representations,[80] which merge omics and imaging data for improved disease characterization, and multimodal subtyping, which enhances phenotypic resolution. Graph-based representations, known for their interpretability and expressiveness, will play a key role in advancing core ML methodologies. Notably, network analysis has been described as a “grand unifier” in biomedical data science, underscoring its potential in HFpEF research.[81]

Identifying clinically relevant HFpEF subtypes remains a challenge, as prior subgroup analyses based on conventional parameters have yet to yield effective therapeutic targets. Evidence from cancer research suggests that integrating multiple biological measurements before subtyping can yield more consistent and clinically actionable classifications.[82] By applying this principle to HFpEF, we aim to overcome previous limitations and improve phenotyping strategies.

The inclusion of a large, well-characterized cohort, along with comparative groups of patients with HFrEF and healthy controls, strengthens the study’s generalizability and analytical depth. Furthermore, its prospective design and clinically relevant primary outcome measure ensure robust validation of the identified HFpEF subtypes, with the ultimate goal of advancing personalized treatment strategies.

Beyond the HFpEF pathology, it is expected that the integrative methods developed during this project will translate to other cardiovascular conditions and will also be relevant to several MRI radiogenomics studies, such as those involving hepatocellular carcinoma.

Feasibility

The study protocol for this HFpEF project is highly feasible, supported by the multidisciplinary expertise of four main investigators and several project partners, each contributing complementary skills to manage the protocol’s complexity. Ruud van Heeswijk leads a radiology-embedded engineering team at CHUV, ensuring access to advanced MRI technology, secure data storage, and computational resources. Jonas Richiardi heads the translational machine learning laboratory, specializing in medical imaging techniques. Roger Hullin and Philippe Meyer lead the Heart Failure Units at CHUV and HUG, respectively, overseeing nearly 1000 patient cases with HFpEF each year. Each investigator directs 1 of 3 Work Packages: van Heeswijk (MRI), Richiardi (ML), and Hullin and Meyer (clinical study). Defined roles and collaborative structures across teams ensure effective data handling, patient recruitment, and ethical compliance, with research nurses in Hullin’s and Meyer’s units managing recruitment and follow-up. In addition, project partners provide required expertise, for example in statistical genetics (Zoltan Kutalik and team), metabolomics (Aurélien Thomas and team), transcriptomics (Julien Marquis and team), advanced cardiac MRI (Matthias Stuber and team), clinical thoracic and abdominal imaging (Jean-Paul Vallée and team), and 4-dimensional flow (Jean-François Deux). The project is also supported by the Clinical Trial Unit at CHUV, ensuring methodological rigor and regulatory compliance. This well-integrated approach provides the necessary capabilities to address the complexities of HFpEF phenotyping and ensures the feasibility of recruitment, data acquisition, and analysis.

Strengths and Limitations

As an observational study, our work is limited by its inability to establish causal relationships between identified HFpEF subtypes and outcomes. Additionally, for resource and logistical reasons, follow-up is limited to 1 year and potential medium- and longer- term outcomes will not be observed.

Our inclusion and exclusion criteria may limit the representativeness of the sample, in particular with respect to comorbidities, which may be more prevalent in the general population with HFpEF than in our sample. Likewise, although the study is already multicentric, its focus on Western Switzerland limits the representativeness of our sample on a wider geographical scale. However, Switzerland is one of the most multicultural countries in Europe, with an estimated 40% of the population having a migration background (either foreign nationals or Swiss-born individuals with foreign-born parents). Although the control group and group with HFrEF are relatively small, they are not intended for detailed subgroup analyses but rather as comparator cohorts. The primary discovery aim of the study lies within the group with HFpEF. With respect to outcomes, assuming a 12-month cardiovascular mortality rate of 15% and a rehospitalization rate of 50% within HFpEF, we anticipate approximately 75 deaths and 250 rehospitalizations. Models will be evaluated both in UKB and in HeartMagic, using cross-validation and independent training/testing schemes. Even under conservative assumptions (eg, sensitivity of 70% for mortality classification), the lower bound of the 95% CI remains well above chance, supporting the adequacy of the planned sample size for biomarker discovery and validation.

A further limitation is that the analytical methods developed using UKB data may not directly transfer to the HeartMagic cohort, given the differences in study populations, imaging modalities, and health care systems. Nevertheless, evidence from cardiovascular imaging and other application domains[83] shows that leveraging external data sets for hypothesis generation and model development can improve performance and robustness in smaller, disease-specific cohorts. UKB imaging data are already multicentric, which facilitates the learning of machine-independent features and supports generalization across settings.

The reliance on advanced imaging and molecular techniques may limit reproducibility in settings without similar resources, and the complexity of data analysis may pose challenges for real-time clinical application.

Despite these limitations, the study's extensive data set could serve as a foundational resource for future HFpEF research, with potential to guide targeted therapeutic developments.

CONCLUSIONS

This multicenter study integrates advanced cardiac and renal MRI with genomic, transcriptomic, and metabolomic profiling to address the clinical and biological heterogeneity of HFpEF. By assembling one of the largest deeply phenotyped HFpEF cohorts to date, HeartMagic aims to identify reproducible disease subtypes linked to distinct mechanisms and outcomes. The use of multimodal machine learning provides a comprehensive framework to refine HFpEF characterization beyond conventional clinical assessment. Comparator groups and integration with UK Biobank data strengthen analytic robustness and enable external validation. Although follow-up is limited to one year, expected event rates will support outcome-focused analyses and biomarker discovery. The methodological developments, including graph-based and transformer-based approaches, are designed to generalize to broader cardiovascular populations. Overall, HeartMagic seeks to advance precision medicine in HFpEF and to provide a foundation for future phenotype-guided therapeutic strategies.

ARTICLE INFORMATION

Received May 7, 2025; accepted October 28, 2025.

Affiliations

Cardiology Division, University Hospital of Geneva, Geneva, Switzerland (P.M., C.T.); Cardiology Division, Lausanne University Hospital (CHUV), Lausanne, Switzerland (A.R., P.M., H.L., A.P.P., T.A., R.H.); Department of Radiology, Lausanne University Hospital (CHUV) and University of Lausanne (UNIL), Lausanne, Switzerland (J.B., A.C.O., C.G., P.C., J-B.L., J.R., R.B.v.H.); Radiology Division, Diagnostic Department, Geneva University Hospitals and University of Geneva, Geneva, Switzerland (A.F., J-P.V., J-F.D., L.A.C.); Faculty Unit of Toxicology, CURML, Faculty of Biology and Medicine, University of Lausanne, Lausanne, Switzerland (A.T.); Unit of Forensic Toxicology and Chemistry, CURML, Lausanne and Geneva University Hospitals, Lausanne, Geneva, Switzerland (A.T.); Lausanne Genomic Technologies Facility, University of Lausanne, Lausanne, Switzerland (J.M.); and CIBM Center for Biomedical Imaging, Lausanne and Geneva, Switzerland (J-B.L.).

Acknowledgments

This research is conducted using the UK Biobank Resource under Application Number 80108. Author contributions: Meyer, Richiardi, Hullin, and van Heeswijk wrote the initial draft of the article. All authors significantly revised the article. Van Heeswijk coordinates the study. Meyer and Tillier set up the recruitment and screening in Geneva; Hullin, Richiardi, Rocca, and Abdurashidova set up the recruitment and screening in Lausanne. Rocca set up the coordination between the project partner teams. Rocca, Tillier and Hullin set up the blood sampling and storage. Thomas established the metabolomic analysis. Marquis, Hullin, and Richiardi set up the genotyping and transcriptomics protocol. Poretta and Hullin established the ECG analysis. Meyer and Monney set up the echocardiography protocol. Van Heeswijk, Ledoux, Vallée, Ogier, Crowe, Calarnou, Fatima, and Deux set up the magnetic resonance imaging acquisition, reconstruction, and analysis. Rocca, Tillier, Meyer, and Hullin collected the clinical data. Richiardi, Banus, and Georgantas established the multimodal data integration and analysis procedure.

Sources of Funding

The HeartMagic study is funded by the Swiss National Science Foundation under grant number CRSII5_202276.

Disclosures

Dr Meyer has served on advisory boards and given educational lectures for AstraZeneca, Bayer, Boehringer Ingelheim, Bristol Myers Squibb, and Pfizer. All honoraria have been paid in full to the GEcor Foundation, a private research foundation affiliated with the Division of Cardiology, Geneva University Hospitals.

Supplemental Material

Tables S1–S4

REFERENCES

1. Savarese G, Becher PM, Lund LH, Seferovic P, Rosano GMC, Coats AJS. Global burden of heart failure: a comprehensive and updated review of epidemiology. *Cardiovasc Res*. 2022;118:3272–3287. doi: 10.1093/cvr/cvac013
2. McDonagh TA, Metra M, Adamo M, Gardner RS, Baumbach A, Böhm M, Burri H, Butler J, Čelutkienė J, Chioncel O, et al. ESC guidelines for the diagnosis and treatment of acute and chronic heart failure. *Eur Heart J*. 2021;42:3599–3726. doi: 10.1093/eurheartj/ehab368
3. Bozkurt B, Coats AJS, Tsutsui H, Abdelhamid CM, Adamopoulos S, Albert N, Anker SD, Atherton J, Böhm M, Butler J, et al. Universal definition and classification of heart failure: a report of the Heart Failure Society of America, Heart Failure Association of the European Society of Cardiology, Japanese Heart Failure Society and writing committee of the Universal Definition of heart failure: endorsed by the Canadian Heart Failure Society, Heart Failure Association of India, Cardiac Society of Australia and New Zealand, and Chinese Heart Failure Association. *Eur J Heart Fail*. 2021;23:352–380. doi: 10.1002/ejhf.2115
4. Gerber Y, Weston SA, Redfield MM, Chamberlain AM, Manemann SM, Jiang R, Killian JM, Roger VL. A contemporary appraisal of the heart failure epidemic in Olmsted County, Minnesota, 2000 to 2010. *JAMA Intern Med*. 2015;175:996–1004. doi: 10.1001/jamainternmed.2015.0924
5. Kittleson MM, Panjrath GS, Amancherla K, Davis LL, Deswal A, Dixon DL, Januzzi JL, Yancy CW. ACC expert consensus decision pathway on management of heart failure with preserved ejection fraction: a report of the American College of Cardiology solution set oversight committee. *J Am Coll Cardiol*. 2023;81:1835–1878. doi: 10.1016/j.jacc.2023.03.393
6. Anker SD, Usman MS, Anker MS, Butler J, Böhm M, Abraham WT, Adamo M, Chopra VK, Cicoira M, Cosentino F, et al. Patient phenotype profiling in heart failure with preserved ejection fraction to guide therapeutic decision making. A scientific statement of the Heart Failure Association, the European Heart Rhythm Association of the European Society of Cardiology, and the European Society of Hypertension. *Eur J Heart Fail*. 2023;25:936–955. doi: 10.1002/ejhf.2894
7. Oghina S, Bougouin W, B ézard M, Kharoubi M, Komajda M, Cohen -Solal A, Mebazaa A, Damy T, Bodez D. The impact of patients with cardiac amyloidosis in HFpEF trials. *JACC Heart Fail*. 2021;9:169–178. doi: 10.1016/j.jchf.2020.12.005
8. Redfield MM. Heart failure with preserved ejection fraction. *N Engl J Med*. 2016;375:1868–1877. doi: 10.1056/NEJMcp1511175
9. Lourenço AP, Leite-Moreira AF, Balligand J-L, Bauersachs J, Dawson D, de Boer RA, de Windt LJ, Falcão-Pires I, Fontes-Carvalho R, Franz S, et al. An integrative translational approach to study heart failure with preserved ejection fraction: a position paper from the working group on myocardial function of the European Society of Cardiology. *Eur J Heart Fail*. 2018;20:216–227. doi: 10.1002/ejhf.1059
10. Campbell P, Rutten FH, Lee MM, Hawkins NM, Petrie MC. Heart failure with preserved ejection fraction: everything the clinician needs to know. *Lancet*. 2024;403:1083–1092. doi: 10.1016/S0140-6736(23)02756-3
11. Pfeffer MA, Shah AM, Borlaug BA. Heart failure with preserved ejection fraction in perspective. *Circ Res*. 2019;124:1598–1617. doi: 10.1161/CIRCRESAHA.119.313572
12. Rocca A, Heeswijk RBV, Richiardi J, Meyer P, Hullin R. The cardiomyocyte in heart failure with preserved ejection fraction—victim of its environment? *Cells*. 2022;11:867. doi: 10.3390/cells11050867
13. Shah SJ, Borlaug BA, Kitzman DW, McCulloch AD, Blaxall BC, Agarwal R, Chirinos JA, Collins S, Deo RC, Gladwin MT, et al. Research priorities for heart failure with preserved ejection fraction: National Heart, Lung, and Blood Institute working group summary. *Circulation*. 2020;141:1001–1026. doi: 10.1161/CIRCULATIONAHA.119.041886
14. Anker SD, Butler J, Filippatos G, Ferreira JP, Bocchi E, Böhm M, Brunner-La Rocca H-P, Choi D-J, Chopra V, Chuquiure-Valenzuela E, et al. Empagliflozin in heart failure with a preserved ejection fraction. *N Engl J Med*. 2021;385:1451–1461. doi: 10.1056/NEJMoa2107038
15. Solomon SD, McMurray JJV, Claggett B, de Boer RA, DeMets D, Hernandez AF, Inzucchi SE, Kosiborod MN, Lam CSP, Martinez F, et al. Dapagliflozin in heart failure with mildly reduced or preserved ejection fraction. 2022;387:1089–1098. doi: 10.1056/NEJMoa2206286
16. Solomon SD, McMurray JJV, Vaduganathan M, Claggett B, Jhund PS, Desai AS, Henderson AD, Lam CSP, Pitt B, Senni M, et al. Finerenone in heart failure with mildly reduced or preserved ejection fraction. 2024;391:1475–1485. doi: 10.1056/NEJMoa2407107
17. Cannata A, McDonagh TA. Heart failure with preserved ejection fraction. 2025;392:173–184. doi: 10.1056/NEJMcp2305181
18. Senni M, Paulus WJ, Gavazzi A, Fraser AG, Díez J, Solomon SD, Smiseth OA, Guazzi M, Lam CSP, Maggioni AP, et al. New strategies for heart failure with preserved ejection fraction: the importance of targeted therapies for heart failure phenotypes. *Eur Heart J*. 2014;35:2797–2815. doi: 10.1093/eurheartj/ehu204
19. Patel RB, Shah SJ. Drug targets for heart failure with preserved ejection fraction: a mechanistic approach and review of contemporary clinical trials. *Annu Rev Pharmacol Toxicol*. 2019;59:41–63. doi: 10.1146/annurev-pharmtox-010818-021136
20. Kosiborod MN, Abildstrøm SZ, Borlaug BA, Butler J, Rasmussen S, Davies M, Hovingh GK, Kitzman DW, Lindegaard ML, Møller DV, et al. Semaglutide in patients with heart failure with preserved ejection fraction and obesity. 2023;389:1069–1084. doi: 10.1056/NEJMoa2306963
21. Kosiborod MN, Petrie MC, Borlaug BA, Butler J, Davies MJ, Hovingh GK, Kitzman DW, Møller DV, Treppendahl MB, Verma S, et al. Semaglutide in patients with obesity-related heart failure and type 2 diabetes. 2024;390:1394–1407. doi: 10.1056/NEJMoa2313917
22. Kosiborod MN, Deanfield J, Pratley R, Borlaug BA, Butler J, Davies MJ, Emerson SS, Kahn SE, Kitzman DW, Lingvay I, et al. Semaglutide versus placebo in patients with heart failure and mildly reduced or preserved ejection fraction: a pooled analysis of the SELECT, FLOW, STEP-HFpEF, and STEP-HFpEF DM randomised trials. *Lancet*. 2024;404:949–961. doi: 10.1016/S0140-6736(24)01643-X
23. Packer M, Zile MR, Kramer CM, Baum SJ, Litwin SE, Menon V, Ge J, Weerakkody GJ, Ou Y, Bunck MC, et al. Tirzepatide for heart failure with preserved ejection fraction and obesity. *N Engl J Med*. 2024;392(5):427–437. doi: 10.1056/NEJMoa2410027
24. Di Sopra L, Piccini D, Coppo S, Stuber M, Yerly J. An automated approach to fully self-gated free-running cardiac and respiratory motion-resolved 5D whole-heart MRI. *Magn Reson Med*. 2019;82:2118–2132. doi: 10.1002/mrm.27898
25. Deo RC. Machine learning in medicine. *Circulation*. 2015;132:1920–1930. doi: 10.1161/CIRCULATIONAHA.115.001593
26. Pieske B, Tschöpe C, de Boer RA, Fraser AG, Anker SD, Donal E, Edelmann F, Fu M, Guazzi M, Lam CSP, et al. How to diagnose heart failure with preserved ejection fraction: the HFA-PEFF diagnostic algorithm: a consensus recommendation from the Heart Failure Association (HFA) of the European Society of Cardiology (ESC). *Eur Heart J*. 2019;40:3297–3317. doi: 10.1093/eurheartj/ehz641
27. Svensson J, Eising S, Hougaard DM, Mortensen HB, Skogstrand K, Simonsen LB, Carstensen B, Nilsson A, Lernmark Å, Pociot F, et al. Few differences in cytokines between patients newly diagnosed with type 1 diabetes and their healthy siblings. *Hum Immunol*. 2012;73:1116–1126. doi: 10.1016/j.humimm.2012.07.337
28. Kowalczuk L, Matet A, Dor M, Bararpour N, Daruich A, Dirani A, Behar-Cohen F, Thomas A, Turck N. Proteome and metabolome of subretinal fluid in central serous chorioretinopathy and Rhegmatogenous retinal detachment: a pilot case study. *Transl Vis Sci Technol*. 2018;7:3. doi: 10.1167/tvst.7.1.3
29. Ivanisevic J, Thomas A. Metabolomics as a tool to understand pathophysiological processes. *Methods Mol Biol*. 2018;1730:3–28. doi: 10.1007/978-1-4939-7592-1_1
30. Dunn WB, Broadhurst D, Begley P, Zelena E, Francis-McIntyre S, Anderson N, Brown M, Knowles JD, Halsall A, Haselden JN, et al. Procedures for large-scale metabolic profiling of serum and plasma using gas chromatography and liquid chromatography coupled to mass spectrometry. *Nat Protoc*. 2011;6:1060–1083. doi: 10.1038/nprot.2011.335

31. Fan S, Kind T, Cajka T, Hazen SL, Tang WHW, Kaddurah-Daouk R, Irvin MR, Arnett DK, Barupal DK, Fiehn O. Systematic error removal using random forest for normalizing large-scale untargeted Lipidomics data. *Anal Chem*. 2019;91:3590–3596. doi: 10.1021/acs.analchem.8b05592
32. Magliocco G, Desmeules J, Matthey A, Quirós-Guerrero LM, Bararpour N, Joye T, Marcourt L, Queiroz EF, Wolfender J-L, Gloor Y, et al. Metabolomics reveals biomarkers in human urine and plasma to predict cytochrome P450 2D6 (CYP2D6) activity. *Br J Pharmacol*. 2021;178:4708–4725. doi: 10.1111/bph.15651
33. Porcu E, Gilardi F, Darrous L, Yengo L, Bararpour N, Gasser M, Marques-Vidal P, Froguel P, Waeber G, Thomas A, et al. Triangulating evidence from longitudinal and Mendelian randomization studies of metabolomic biomarkers for type 2 diabetes. *Sci Rep*. 2021;11:6197. doi: 10.1038/s41598-021-85684-7
34. Wolfender J-L, Marti G, Thomas A, Bertrand S. Current approaches and challenges for the metabolite profiling of complex natural extracts. *J Chromatogr A*. 2015;1382:136–164. doi: 10.1016/j.chroma.2014.10.091
35. Dührkop K, Fleischauer M, Ludwig M, Aksenov AA, Melnik AV, Meusel M, Dorrestein PC, Rousu J, Böcker S. SIRIUS 4: a rapid tool for turning tandem mass spectra into metabolite structure information. *Nat Methods*. 2019;16:299–302. doi: 10.1038/s41592-019-0344-8
36. Dührkop K, Nothias L-F, Fleischauer M, Reher R, Ludwig M, Hoffmann MA, Petras D, Gerwick WH, Rousu J, Dorrestein PC, et al. Systematic classification of unknown metabolites using high-resolution fragmentation mass spectra. *Nat Biotechnol*. 2021;39:462–471. doi: 10.1038/s41587-020-0740-8
37. Wingett SW, Andrews S. FastQ screen: a tool for multi-genome mapping and quality control. *F1000Res*. 2018;7:1338. doi: 10.12688/f1000research.15931.1
38. Extramiana F, Laporte P-L, Vaglio M, Denjoy I, Maison-Blanche P, Badilini F, Leenhardt A. Computerized automated algorithm-based analyses of digitized paper ECGs in Brugada syndrome. *J Electrocardiol*. 2021;69:61–66. doi: 10.1016/j.jelectrocard.2021.09.009
39. Kligfield P, Badilini F, Denjoy I, Babaeizadeh S, Clark E, De Bie J, Devine B, Extramiana F, Generali G, Gregg R, et al. Comparison of automated interval measurements by widely used algorithms in digital electrocardiographs. *Am Heart J*. 2018;200:1–10. doi: 10.1016/j.ahj.2018.02.014
40. Badilini F, Libretti G, Vaglio M. Automated JTpeak analysis by BRAVO. *J Electrocardiol*. 2017;50:752–757. doi: 10.1016/j.jelectrocard.2017.07.010
41. Georgantas C, Kutalik Z, Richiardi J. Deep learning for polygenic risk prediction. 2024 2024.04.19.24306079.
42. Mitchell C, Rahko PS, Blauwet LA, Canaday B, Finstuen JA, Foster MC, Horton K, Ogunyankin KO, Palma RA, Velazquez EJ. Guidelines for performing a comprehensive transthoracic echocardiographic examination in adults: recommendations from the American Society of Echocardiography. *J Am Soc Echocardiogr*. 2019;32:1–64. doi: 10.1016/j.echo.2018.06.004
43. Lang RM, Badano LP, Mor-Avi V, Afilalo J, Armstrong A, Ernande L, Flachskampf FA, Foster E, Goldstein SA, Kuznetsova T, et al. Recommendations for cardiac chamber quantification by echocardiography in adults: an update from the American Society of Echocardiography and the European Association of Cardiovascular Imaging. *Eur Heart J Cardiovasc Imaging*. 2015;16:233–271. doi: 10.1093/ehjci/jev014
44. Nagueh SF, Smiseth OA, Appleton CP, Byrd BF, Dokainish H, Edvardsen T, Flachskampf FA, Gillebert TC, Klein AL, Lancellotti P, et al. Recommendations for the evaluation of left ventricular diastolic function by echocardiography: an update from the American Society of Echocardiography and the European Association of Cardiovascular Imaging. *Eur Heart J Cardiovasc Imaging*. 2016;17:1321–1360. doi: 10.1093/ehjci/jew082
45. Smiseth OA, Morris DA, Cardim N, Cikes M, Delgado V, Donal E, Flachskampf FA, Galderisi M, Gerber BL, Gimelli A, et al. Multimodality imaging in patients with heart failure and preserved ejection fraction: an expert consensus document of the European Association of Cardiovascular Imaging. *Eur Heart J Cardiovasc Imaging*. 2022;23:e34–e61. doi: 10.1093/ehjci/jeab154
46. Coats AJS, Anker SD, Baumbach A, Alfieri O, Von Bardeleben RS, Bauersachs J, Bax JJ, Boveda S, Čelutkienė J, Cleland JG, et al. The management of secondary mitral regurgitation in patients with heart failure: a joint position statement from the Heart Failure Association (HFA), European Association of Cardiovascular Imaging (EACVI), European Heart Rhythm Association (EHRA), and European Association of Percutaneous Cardiovascular Interventions (EAPCI) of the ESC. *Eur Heart J*. 2021;42:1254–1269. doi: 10.1093/eurheartj/ehab086
47. Baumgartner H, Hung J, Bermejo J, Chambers JB, Edvardsen T, Goldstein S, Lancellotti P, LeFevre M, Miller F, Otto CM. Recommendations on the echocardiographic assessment of aortic valve stenosis: a focused update from the European Association of Cardiovascular Imaging and the American Society of Echocardiography. *Eur Heart J Cardiovasc Imaging*. 2017;18:254–275. doi: 10.1093/ehjci/jew335
48. Lancellotti P, Pibarot P, Chambers J, La Canna G, Pepi M, Dulgheru R, Dweck M, Delgado V, Garbi M, Vannan MA, et al. Multi-modality imaging assessment of native valvular regurgitation: an EACVI and ESC council of valvular heart disease position paper. *Eur Heart J Cardiovasc Imaging*. 2022;23:e171–e232. doi: 10.1093/ehjci/jeab253
49. Christensen RH, Lundgren T, Stenvinkel P, Brismar TB. Renal volumetry with magnetic resonance imaging. *Acta Radiol Open*. 2017;6:2058460117731120. doi: 10.1177/2058460117731120
50. Milani B, Ansaloni A, Sousa-Guimaraes S, Vakilzadeh N, Piskunowicz M, Vogt B, Stuber M, Burnier M, Pruijm M. Reduction of cortical oxygenation in chronic kidney disease: evidence obtained with a new analysis method of blood oxygenation level-dependent magnetic resonance imaging. *Nephrol Dial Transplant*. 2017;32:2097–2105. doi: 10.1093/ndt/gfw362
51. Calarnou P, Ogier AC, Roy CW, Rocca A, Abdurashidova T, Ledoux J-B, Hullin R, Bustin A, Yerly J, van Heeswijk RB. Navigator-gated free-breathing 2D radial cardiac joint T1-T2 mapping. *Magn Reson Med*. 2025;94:1577–1591. doi: 10.1002/mrm.30588
52. Vincenti G, Monney P, Chaptinel J, Rutz T, Coppo S, Zenge MO, Schmidt M, Nadar MS, Piccini D, Chèvre P, et al. Compressed sensing single–breath-hold CMR for fast quantification of LV function, volumes, and mass. *JACC Cardiovasc Imaging*. 2014;7:882–892. doi: 10.1016/j.jcmg.2014.04.016
53. Xue H, Brown LAE, Nielles-Vallespin S, Plein S, Kellman P. Automatic in-line quantitative myocardial perfusion mapping: processing algorithm and implementation. *Magn Reson Med*. 2020;83:712–730. doi: 10.1002/mrm.27954
54. Vasu S, Bandettini WP, Hsu L-Y, Kellman P, Leung S, Mancini C, Shanbhag SM, Wilson J, Booker OJ, Arai AE. Regadenoson and adenosine are equivalent vasodilators and are superior than dipyridamole- a study of first pass quantitative perfusion cardiovascular magnetic resonance. 2013;15:85. doi: 10.1186/1532-429X-15-85
55. Ma LE, Markl M, Chow K, Huh H, Forman C, Vali A, Greiser A, Carr J, Schnell S, Barker AJ, et al. Aortic 4D flow MRI in 2 minutes using compressed sensing, respiratory controlled adaptive k-space reordering, and inline reconstruction. *Magn Reson Med*. 2019;81:3675–3690. doi: 10.1002/mrm.27684
56. Calarnou P, Ogier AC, Roy CW, Ledoux J-B, Rocca A, Pruijm M, Hullin R, Vallée J-P, Yerly J, van Heeswijk RB. Navigator-gated free-breathing joint T1-T2 mapping of the kidney. *medRxiv*. 2025;2025.08.17.25333832.
57. Piccini D, Littmann A, Nielles-Vallespin S, Zenge MO. Spiral phyllotaxis: the natural way to construct a 3D radial trajectory in MRI. *Magn Reson Med*. 2011;66:1049–1056. doi: 10.1002/mrm.22898
58. Montón Quesada I, Ogier AC, Ishida M, Takafuji M, Ito H, Sakumu H, Romanin L, Roy CW, Prša M, Richiardi J, et al. Self-gated free-running 5D whole-heart MRI using blind source separation for automated cardiac motion extraction. *Magn Reson Med*. 2025;93(3):961–974. doi: 10.1002/mrm.30322
59. Ogier AC, Montón Quesada I, Sieber X, Calarnou P, Ledoux J-B, Milani B, Schwitter J, Roy CW, Yerly J, Stuber M, et al. Free-running 5D whole-heart MRI for isotropic cardiac function measurements at 3T without contrast agents. *Magn Reson Med*. 2025;93(6):2386–2400. doi: 10.1002/mrm.30469
60. Feng L, Coppo S, Piccini D, Yerly J, Lim RP, Masci PG, Stuber M, Sodickson DK, Otazo R. 5D whole-heart sparse MRI. *Magn Reson Med*. 2018;79:826–838. doi: 10.1002/mrm.26745
61. Reddy YNV, Carter RE, Obokata M, Redfield MM, Borlaug BA. A simple, evidence-based approach to help guide diagnosis of heart failure with preserved ejection fraction. *Circulation*. 2018;138:861–870. doi: 10.1161/CIRCULATIONAHA.118.034646
62. Zhao S, Li C-I, Guo Y, Sheng Q, Shyr Y. RnaSeqSampleSize. 2017.
63. Aslam I, Aamir F, Kassai M, Crowe LA, Poletti P-A, Seigneux SD, Moll S, Berchtold L, Vallée J-P. Validation of automatically measured T1 map cortico-medullary difference (ΔT1) for eGFR and fibrosis assessment in allograft kidneys. *PLoS One*. 2023;18:e0277277. doi: 10.1371/journal.pone.0277277
64. Kowallick JT, Morton G, Lamata P, Jogiya R, Kutty S, Hasenfuß G, Lotz J, Nagel E, Chiribiri A, Schuster A. Quantification of atrial dynamics

using cardiovascular magnetic resonance: inter-study reproducibility. *J Cardiovasc Magn Reson*. 2015;17:36. doi: 10.1186/s12968-015-0140-2
65. Dellegrottaglie S, Sanz J, Poon M, Viles-Gonzalez JF, Sulica R, Goyenechea M, Macaluso F, Fuster V, Rajagopalan S. Pulmonary hypertension: accuracy of detection with left ventricular septal-to–free wall curvature ratio measured at cardiac MR. *Radiology*. 2007;243:63–69. doi: 10.1148/radiol.2431060067
66. Cerqueira MD, Weissman NJ, Dilsizian V, Jacobs AK, Kaul S, Laskey WK, Pennell DJ, Rumberger JA, Ryan T, Verani MS. Standardized myocardial segmentation and nomenclature for tomographic imaging of the heart. *Circulation*. 2002;105:539–542. doi: 10.1161/hc0402.102975
67. Vargas-Barron J, Roldan J, Espinola-Zavaleta N, Romero-Cárdenas A, Keirns C, López-Meneses M, Martínez-Ríos MA. Prognostic implications of right atrial ischemic dysfunction in patients with biventricular inferior infarction: transesophageal echocardiographic analysis. *Echocardiography*. 2001;18:105–112. doi: 10.1046/j.1540-8175.2001.00105.x
68. Kellman P, Hansen MS, Nielles-Vallespin S, Nickander J, Themudo R, Ugander M, Xue H. Myocardial perfusion cardiovascular magnetic resonance: optimized dual sequence and reconstruction for quantification. *J Cardiovasc Magn Reson*. 2016;19:43. doi: 10.1186/s12968-017-0355-5
69. Georgantas C, Banus J, Hullin R, Richiardi J. Systematic estimation of treatment effect on hospitalization risk as a drug repurposing screening method. *Biocomputing 2024*. Kohala Coast, Hawaii, USA: World Scientific; 2023:232–246.
70. Truong VQ, Woerner JA, Cherlin TA, Bradford Y, Lucas AM, Okeh CC, Shivakumar MK, Hui DH, Kumar R, Pividori M, et al. Quality control procedures for genome-wide association studies. *Curr Protoc*. 2022;2:e603. doi: 10.1002/cpz1.603
71. Privé F, Aschard H, Ziyatdinov A, Blum MGB. Efficient analysis of large-scale genome-wide data with two R packages: bigstatsr and bigsnpr. *Bioinformatics*. 2018;34:2781–2787. doi: 10.1093/bioinformatics/bty185
72. Graubert A, Aguet F, Ravi A, Ardlie KG, Getz G. RNA-SeQC 2: efficient RNA-seq quality control and quantification for large cohorts. *Bioinformatics*. 2021;37:3048–3050. doi: 10.1093/bioinformatics/btab135
73. Patro R, Duggal G, Love MI, Irizarry RA, Kingsford C. Salmon provides fast and bias-aware quantification of transcript expression. *Nat Methods*. 2017;14:417–419. doi: 10.1038/nmeth.4197
74. Dobin A, Davis CA, Schlesinger F, Drenkow J, Zaleski C, Jha S, Batut P, Chaisson M, Gingeras TR. STAR: ultrafast universal RNA-seq aligner. *Bioinformatics*. 2013;29:15–21. doi: 10.1093/bioinformatics/bts635
75. Putri GH, Anders S, Pyl PT, Pimanda JE, Zanini F. Analysing high-throughput sequencing data in python with HTSeq 2.0. Boeva V, ed. *Bioinformatics*. 2022;38:2943–2945. doi: 10.1093/bioinformatics/btac166
76. Zitnik M, Nguyen F, Wang B, Leskovec J, Goldenberg A, Hoffman MM. Machine learning for integrating data in biology and medicine: principles, practice, and opportunities. *Inform Fusion*. 2019;50:71–91. doi: 10.1016/j.inffus.2018.09.012
77. Prasser F, Kohlmayer F, Lautenschläger R, Kuhn KA. ARX--A comprehensive tool for anonymizing biomedical data. *AMIA Symp*. 2014;2014:984–993.
78. Ziegenhain C, Sandberg R. BAMboozle removes genetic variation from human sequence data for open data sharing. *Nat Commun*. 2021;12:6216. doi: 10.1038/s41467-021-26152-8
79. Gürsoy G, Emani P, Brannon CM, Jolanki OA, Harmanci A, Strattan JS, Cherry JM, Miranker AD, Gerstein M. Data sanitization to reduce private information leakage from functional genomics. *Cell*. 2020;183:905–917. e16. doi: 10.1016/j.cell.2020.09.036
80. Holzinger A, Haibe-Kains B, Jurisica I. Why imaging data alone is not enough: AI-based integration of imaging, omics, and clinical data. *Eur J Nucl Med Mol Imaging*. 2019;46:2722–2730. doi: 10.1007/s00259-019-04382-9
81. McGillivray P, Clarke D, Meyerson W, Zhang J, Lee D, Gu M, Kumar S, Zhou H, Gerstein M. Network analysis as a grand unifier in biomedical data science. *Annu Rev Biomed Data Sci*. 2018;1:153–180. doi: 10.1146/annurev-biodatasci-080917-013444
82. Cavalli FMG, Remke M, Rampasek L, Peacock J, Shih DJH, Luu B, Garzia L, Torchia J, Nor C, Morrissy AS, et al. Intertumoral heterogeneity within medulloblastoma subgroups. *Cancer Cell*. 2017;31:737–754. e6. doi: 10.1016/j.ccell.2017.05.005
83. Aung N, Vargas JD, Yang C, Cabrera CP, Warren HR, Fung K, Tzanis E, Barnes MR, Rotter JI, Taylor KD, et al. Genome-wide analysis of left ventricular image-derived phenotypes identifies fourteen loci associated with cardiac morphogenesis and heart failure development. *Circulation*. 2019;140:1318–1330. doi: 10.1161/CIRCULATIONAHA.119.041161